Oxoazides

Deutsche Ausgabe: DOI: 10.1002/ange.201504629
Internationale Ausgabe: DOI: 10.1002/anie.201504629

The First Molybdenum(VI) and Tungsten(VI) Oxoazides $MO_2(N_3)_2$, $MO_2(N_3)_2{\cdot}2\,CH_3CN$, $(bipy)MO_2(N_3)_2$, and $[MO_2(N_3)_4]^{2-}$ (M = Mo, W)**

Ralf Haiges, Juri Skotnitzki, Zongtang Fang, David A. Dixon, and Karl O. Christe*

Dedicated to Ross I. Wagner on the occasion of his 90th birthday

Abstract: *Molybdenum(VI) and tungsten(VI) dioxodiazide, $MO_2(N_3)_2$ (M = Mo, W), were prepared through fluoride–azide exchange reactions between MO_2F_2 and Me_3SiN_3 in SO_2 solution. In acetonitrile solution, the fluoride–azide exchange resulted in the isolation of the adducts $MO_2(N_3)_2{\cdot}2\,CH_3CN$. The subsequent reaction of $MO_2(N_3)_2$ with 2,2′-bipyridine (bipy) gave the bipyridine adducts $(bipy)MO_2(N_3)_2$. The hydrolysis of $(bipy)MoO_2(N_3)_2$ resulted in the formation and isolation of $[(bipy)MoO_2N_3]_2O$. The tetraazido anions $[MO_2(N_3)_4]^{2-}$ were obtained by the reaction of $MO_2(N_3)_2$ with two equivalents of ionic azide. Most molybdenum(VI) and tungsten(VI) dioxoazides were fully characterized by their vibrational spectra, impact, friction, and thermal sensitivity data and, in the case of $(bipy)MoO_2(N_3)_2$, $(bipy)WO_2(N_3)_2$, $[PPh_4]_2[MoO_2(N_3)_4]$, $[PPh_4]_2[WO_2(N_3)_4]$, and $[(bipy)MoO_2N_3]_2O$ by their X-ray crystal structures.*

Polyazides are highly energetic compounds that have attracted considerable interest as potential high-energy-density materials (HEDM).[1] Because of their highly endothermic nature, polyazido compounds are usually explosive and very sensitive to shock, rendering the synthesis of molecules with a large number of azido groups difficult. The chemistry of high-oxidation-state metal polyazides is more challenging than the one of lower-oxidation-state metals because the increased oxidation potential of the central metal atom results in polyazido compounds with increased sensitivity and explosiveness.[2] The stabilization of neutral polyazides by either anion or adduct formation has been well established in recent years.[3] Another, less common approach for the stabilization of high-oxidation-state metal azides is the introduction of oxygen atoms in order to reduce the oxidation potential of the central metal atom.[4] The oxidation potential of a metal oxohalide or metal dioxohalide is lower than that of the corresponding oxygen-free metal halide with the metal in the same oxidation state. The binary polyazides $Mo(N_3)_6$, $W(N_3)_6$, $[PPh_4][Mo(N_3)_7]$, and $[PPh_4][W(N_3)_7]$ have been described as very treacherous, extremely shock- and temperature-sensitive compounds that explode violently when warmed toward room temperature.[5] The only structurally characterized polyazides of molybdenum and tungsten are $W(N_3)_6$ and $[NMo(N_3)_4]^-$.[5,6] To the best of our knowledge, no molybdenum(VI) or tungsten(VI) oxopolyazide have been structurally characterized so far.

In agreement with our previously reported syntheses of $W(N_3)_6$ and $Mo(N_3)_6$,[5] the reaction of molybdenum or tungsten dioxodifluoride with an excess of trimethylsilyl azide in acetonitrile solution at −20 °C resulted in a complete fluoride–azide exchange and the formation of dark maroon to black (M = Mo) or red (M = W) solutions. When the volatile compounds (CH_3CN, Me_3SiF, and excess Me_3SiN_3) were pumped off, first at −20 °C and then at ambient temperature, the corresponding metal dioxodiazides were obtained as the acetonitrile adducts $MO_2(N_3)_2{\cdot}2\,CH_3CN$ in the form of black (molybdenum) or red (tungsten), slightly tacky solids [Eq. (1), M = Mo, W].

$$MO_2F_2 + 2\,Me_3SiN_3 \xrightarrow[-2\,Me_3SiF]{CH_3CN} MO_2(N_3)_2 \cdot 2\,CH_3CN \qquad (1)$$

The acetonitrile adducts are stable at ambient temperature but are sensitive to impact and friction and explode upon fast heating with an open flame. All attempts of growing single crystals of both acetonitrile adducts $MoO_2(N_3)_2{\cdot}2\,CH_3CN$ and $WO_2(N_3)_2{\cdot}2\,CH_3CN$ that are suitable for X-ray crystal structure determination, were unsuccessful. The composition of the compounds was established by the observed material balances, their vibrational spectra (see the Supporting Information; SI), and their conversion into the adducts $(bipy)MO_2(N_3)_2$ and anions $[MO_2(N_3)_4]^{2-}$. The reaction of the metal dioxodifluorides with trimethylsilyl azide in SO_2 solution at −20 °C, resulted again in a complete fluoride–azide exchange and the formation of dark maroon to black

[*] Prof. Dr. R. Haiges, J. Skotnitzki, Prof. Dr. K. O. Christe
Loker Hydrocarbon Research Institute and Department of Chemistry, University of Southern California
Los Angeles, CA 90089-1661 (USA)
E-mail: haiges@usc.edu
Z. Fang, Prof. Dr. D. A. Dixon
Department of Chemistry, The University of Alabama
Tuscaloosa, AL 35487 (USA)

[**] The Office of Naval Research (ONR) and the Defense Threat Reduction Agency (DTRA) funded this work. The National Science Foundation supported the X-ray diffractometer (NSF CRIF 1048807). We thank Prof. G. K. S. Prakash and Drs. W. Wilson, as well as G. B.-Chabot, P. Deokar, and A. Baxter for their help and stimulating discussions. The calculations were supported by the Chemical Sciences, Geosciences and Biosciences Division, Office of Basic Energy Sciences, U.S. Department of Energy (DOE) (catalysis center program). D.A.D. thanks the Robert Ramsay Chair Fund of The University of Alabama for support.

Supporting information for this article is available on the WWW under http://dx.doi.org/10.1002/anie.201504629.

(M = Mo) or red (M = W) solutions of $MO_2(N_3)_2$. The neat dioxodiazides $MoO_2(N_3)_2$ and $WO_2(N_3)_2$ were obtained as black (Mo) or red (W) solids that are stable at ambient temperature but very sensitive to friction and impact. The composition of the compounds was established by their vibrational spectra and the observed material balances (see SI)

$$MO_2(N_3)_3 + \text{bipy} \xrightarrow{CH_3CN} (\text{bipy})MO_2(N_3)_2 \quad (2)$$

The 1:1 adducts $(bipy)MO_2(N_3)_2$ (M = Mo, W) were formed quantitatively when the dioxodiazides $MO_2(N_3)_2$ were reacted with 2,2′-bipyridine (bipy) in acetonitrile solution. [Eq. (2)]. Both bipyridine adducts were isolated as impact- and friction-sensitive, brown (Mo) or orange-red (W) crystalline solids and were identified and characterized by their vibrational spectra and X-ray crystal structures. When a solution of $(bipy)MoO_2(N_3)_2$ in acetonitrile was kept in an evacuated thin-walled (0.5 mm wall thickness) FEP reactor for a period of three days, a heterogeneous mixture of a grey amorphous solid and brown crystals was obtained once the solvent was removed. An X-ray crystal structure determination identified the crystalline material as $[(bipy)MO_2N_3]_2O$, which was presumably formed through the hydrolysis of $(bipy)MoO_2(N_3)_2$ with moisture that had diffused into the reactor [Eq. (3)].

$$2\,(\text{bipy})MoO_2(N_3)_3 + H_2O \xrightarrow[-2\,HN_3]{CH_3CN} [(\text{bipy})MoO_2N_3]_2O \quad (3)$$

The $[(bipy)MO_2N_3]_2O$ was identified and characterized solely by its X-ray crystal structure and no attempts were made to further characterize the compound or to identify other hydrolysis products. When the dioxodiazides, $MO_2(N_3)_2$, were reacted with two equivalents of PPh_4N_3 in acetonitrile solution, salts of the corresponding dioxotetraazidometalates, $[PPh_4]_2[MO_2(N_3)_4]$, were formed quantitatively [Eq. (4), M = Mo, W].

$$MO_2(N_3)_3 + 2\,PPh_4N_3 \xrightarrow{CH_3CN} [PPh_4]_2[MO_2(N_3)_4] \quad (4)$$

Both dioxotetraazidometalate(VI) salts were isolated as orange-brown, crystalline solids that were characterized by their vibrational spectra and X-ray crystal structures. The reaction of $MO_2(N_3)_2$ with a single equivalent of PPh_4N_3 did not result in the formation of a $[MO_2(N_3)_3]^-$ salt but a mixture of $[PPh_4]_2[MO_2(N_3)_4]$ and $MO_2(N_3)_2$.

Details of the crystallographic data collection and refinement parameters for the structurally characterized compounds $(bipy)MoO_2(N_3)_2$, $(bipy)WO_2(N_3)_2$, $[PPh_4]_2[MoO_2(N_3)_4]$, and $[PPh_4]_2[MoO_2(N_3)_4]$ are given in the SI. Both bipyridine adducts, $(bipy)MoO(N_3)_2$ and $(bipy)WO(N_3)_2$, crystallize in the triclinic space group $P\bar{1}$ (Figure 1). The solid-state structure contains isolated and well-separated molecules. The shortest intermolecular N···N and Mo···N distances involving azido groups in $(bipy)MoO_2(N_3)_2$ are 3.137(3) Å and 4.292(2) Å, respectively. The shortest intermolecular Mo···O distance is 4.494(2) Å. In $(bipy)WO_2(N_3)_2$, the shortest intermolecular N–N and W–N distances involving azido groups are found at 3.105(3) Å and 4.756(3) Å, respectively. The shortest intermolecular W···O distance is 5.459(2) Å.

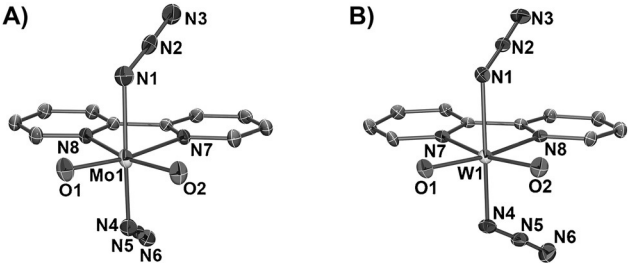

Figure 1. Crystal structure of A) $(bipy)MoO_2(N_3)_2$ and B) $(bipy)WO_2(N_3)_2$. Thermal ellipsoids are shown at the 50% probability level. Hydrogen atoms have been omitted for clarity.

The solid-state structures of the two bipyridine adducts $(bipy)MoO_2(N_3)_2$ and $(bipy)WO_2(N_3)_2$ are very similar but the compounds are not isostructural. For both molecules, the coordination geometry around the central metal atom is derived from a distorted octahedron with the two azido ligands occupying the axial positions. The two nitrogen atoms of the 2,2′-bipyridine ligand and the two oxygen atoms occupy the equatorial positions (Figure 1). The major difference between the two structures is the orientation of the azido ligands, which are quite floppy. It has already been shown that there are usually only minor differences in energy (< 2 kcal mol^{-1}) between different orientations of the N_3-groups in a molecule.[7] Both azido groups in $(bipy)MoO_2(N_3)_2$ and $(bipy)WO_2(N_3)_2$ are pointing away from the oxygen atoms and in the general direction of the bipyridine ligand. However, while one of the azido ligands (N4-N6) in the molybdenum compound is pointing in-between the six-membered rings of the bipyridine ligand, the second one is pointing toward the center of one six-membered ring. The angle between the two N_3-groups is 24.9°. In $(bipy)WO_2(N_3)_2$, both azido groups are rotated relative to their orientation in the molybdenum compound and are pointing in the direction of the same six-membered ring. The angle between the two N_3-groups in the tungsten compound is 22.8°.

The average $Mo–N_{azido}$ distance of 2.060(2) Å in $(bipy)MoO_2(N_3)_2$ is in good agreement with the one observed for the $[Mo(N)(N_3)_4]^-$ anion (2.068(3) Å).[5,6] The observed average Mo–O distance of 1.716(2) Å is considerably larger than the Mo–O distance of 1.682(3) Å found in $(bipy)MoO_2F_2$.[8] In $(bipy)WO_2(N_3)_2$, the observed average $W–N_{azido}$ distance of 2.049(3) Å is larger than the one found for $W(N_3)_6$ (1.978(2) Å)[5] but slightly smaller than the average $Mo–N_{azido}$ distance in $(bipy)MoO_2(N_3)_2$. The observed average W–O distance of 1.729(3) Å is again larger than the one observed (1.67(1) Å) in the corresponding metal fluoride $(bipy)WO_2F_2$.[9] The N–N distances in the azido ligands of both bipyridine adducts are 1.214(3) Å (Mo) and 1.209(5) Å (W) for the internal N–N bond, and 1.143(2) Å (Mo) and 1.148(5) Å (W) for the external azide bond, which are typical values for covalent azides. The tetraphenylphosphonium dioxoazido salts $[PPh_4]_2[MoO_2(N_3)_4]$ and $[PPh_4]_2[WO_2(N_3)_4]$ crystallize in the monoclinic space group $P2_1/c$ with four formula units in the unit cell. Both crystal structures consist of

well-separated cations and anions. The shortest cation–anion distances between nonhydrogen atoms is 3.072(5) Å (Mo compound) and 3.040(4) Å (W compound). The shortest Mo···N and N···N distances between individual anions in $[PPh_4]_2[MoO_2(N_3)_4]$ were 7.512(3) Å and 6.182(5) Å, respectively. In $[PPh_4]_2[WO_2(N_3)_4]$, the closest W···N and N···N distances between individual anions are 7.526(4) Å and 5.011(6) Å. The structures of both dioxotetraazido metallate-(IV) anions, $[MoO_2(N_3)_4]^{2-}$ and $[WO_2(N_3)_4]^{2-}$ are derived from a pseudo-octahedral ligand arrangement around the central metal atom (Figure 2) and are similar to the structures

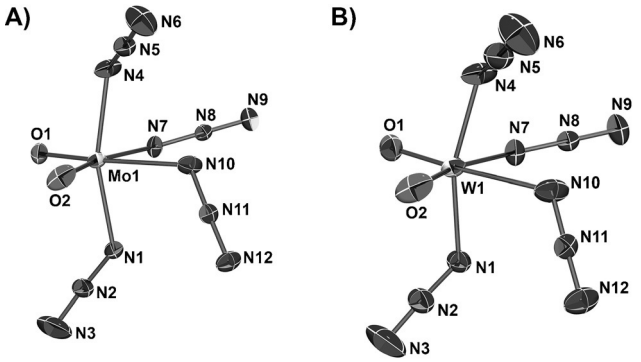

Figure 2. The anion in the crystal structure of A) $[PPh_4]_2[MoO_2(N_3)_4]$ and B) $[PPh_4]_2[WO_2(N_3)_4]$. Thermal ellipsoids are shown at the 50% probability level.

of $(bipy)MO_2(N_3)_2$ (M = Mo, W) that have been discussed before. Two axial and two equatorial azido ligands coordinate the central metal atom. Two equatorial oxygen atoms in *cis* configuration complete the pseudo-octahedral environment. The M–N distances for the equatorial azido ligands (Mo: 2.190(2) and 2.275(2) Å; W: 2.183(2) and 2.255(3) Å) are noticeable larger than the ones of the axial azido ligands (Mo: 2.078(2) and 2.102(2) Å; W: 2.068(3) and 2.085(3) Å). The Mo–O distances are 1.713(1) and 1.727(2) Å and the W–O distances are 1.730(2) and 1.736(2) Å. For both species, the adducts $(bipy)MO_2(N_3)_2$ and the anions $[MO_2(N_3)_4]^{2-}$, the observed $M–N_{azide}$ distances are larger for molybdenum than for tungsten whereas the molybdenum–oxygen distances were smaller than the ones between tungsten and oxygen. The average N–N distances in the azido ligands of 1.141(4) Å for the external azide bond and 1.202(4) Å for the internal bond are typical for covalent azides.

The hydrolysis product $[(bipy)MoO_2N_3]_2O$ crystallizes in the monoclinic space group $P2_1/c$ with four symmetry-related molecules per unit cell. The solid-state structure consists of isolated $[(bipy)MoO_2N_3]_2O$ molecules. The shortest intermolecular Mo···O, Mo···N_{azide}, and N_{azide}···N_{azide} distances are 4.256(2) Å, 4.790(2) Å, and 4.455(4) Å, respectively. Each molecule consists of two oxygen-bridged $(bipy)MoO_2N_3$ units with a distorted pseudo-octahedral coordinated molybdenum atom (Figure 3). The bipyridine ligand and two oxygen atoms coordinate the metal in the equatorial positions. One azido ligand and the bridging oxygen atom occupy the axial positions. The average $Mo–N_{azide}$ distance of 2.105(2) Å is larger than the one found in $(bipy)MoO_2(N_3)_2$.

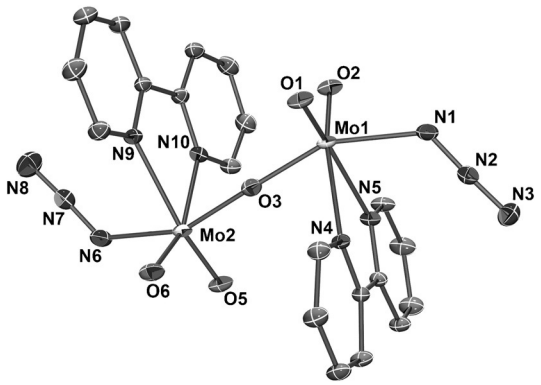

Figure 3. Crystal structure of $[(bipy)MoO_2N_3]_2O$. Thermal ellipsoids are shown at the 50% probability level. Hydrogen atoms have been omitted for clarity.

Quantum chemical calculations were performed at the B3LYP//DZVP2/cc-pVDZ-PP and SVWN5//DZVP2/cc-pVDZ-PP density functional theory (DFT) levels for the metal dioxoazide species $MO_2(N_3)_2$, $(bipy)MO_2(N_3)_2$, $[MO_2(N_3)_3]^-$, and $[MO_2(N_3)_4]^{2-}$, as well as the acetonitrile adducts $MO_2(N_3)_2{\cdot}CH_3CN$ and $MO_2(N_3)_2{\cdot}2\,CH_3CN$ (M = Mo, W). The local DFT functional was included as it often gives better geometries for transition metal compounds than do hybrid functionals such as B3LYP. The obtained geometries and calculated vibrational frequencies and intensities are given in the SI. A summary of the optimized is given in Figure S1 in the SI.

The B3LYP and SVWN5 functionals predict for $MO_2(N_3)_2$, $[MO_2(N_3)_3]^-$, and $[MO_2(N_3)_4]^{2-}$ single minimum-energy structures (Figure 4). Two different structures were found for

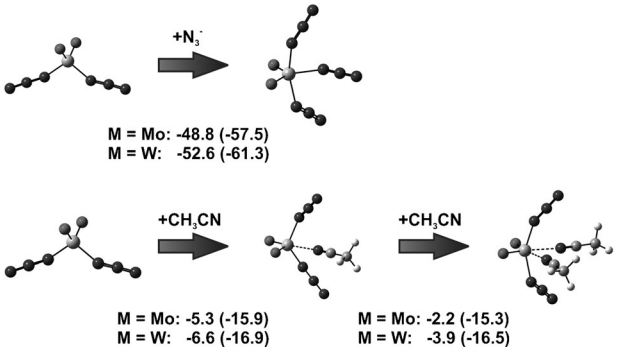

Figure 4. Reaction energies [kcal mol^{-1}] for the addition of N_3^- or CH_3CN to $MO_2(N_3)_2$ (M = Mo, W) calculated at the B3LYP//aug-cc-pVDZ/aug-cc-pVDZ-PP level. Values given in parenthesis were calculated at the MP2//aug-cc-pVDZ/aug-cc-pVDZ-PP level.

the adducts $(bipy)MO_2(N_3)_2$ and $MO_2(N_3)_2{\cdot}CH_3CN$, whereas three minimum structures were found for $MO_2(N_3)_2{\cdot}2\,CH_3CN$. The optimized structures show that $MoO_2(N_3)_2$ and $WO_2(N_3)_2$ have the expected pseudo-tetrahedral geometry of C_2 symmetry. The predicted minimum energy structures for $[MoO_2(N_3)_3]^-$ and $[WO_2(N_3)_3]^-$ are of C_s symmetry. The average Mo–N and W–N distances in $[MO_2$-

$(N_3)_3]^-$ are slightly larger (0.115–0.129 Å) than the ones of the corresponding neutral diazido compounds $MO_2(N_3)_2$, indicating an increased ionic character of the azido ligands. The predicted minimum-energy structures of the dianions $[MO_2(N_3)_4]^{2-}$ are pseudo-octahedral with the two O atoms *cis* to each other (Figure S1) and are in reasonable agreement with the ones observed in the X-ray crystal structures. Two different structures of C_s and C_2 symmetry with different orientations of the azido ligands were found for the bipyridine adducts $(bipy)MO_2(N_3)_2$ (Figure S1). Both structures are comparable in energy, demonstrating the conformational flexibility of the azido groups. The addition of an N_3^- to $MO_2(N_3)_2$ and formation of the pseudo-trigonal-bipyramidal structure of $[MO_2(N_3)_3]^-$ is a significantly exothermic process in the gas phase (Figure 4). Additional single-point calculations were performed at the MP2 level[10] with the aug-cc-pVDZ/aug-cc-pVDZ-PP(metal) basis sets[11] because the MP2 method can handle weak interactions better than density functional theory. The MP2 values are more exothermic than the DFT values but show the same qualitative trend with the stronger Lewis acid W^{VI} site[12] having the more exothermic reaction. The addition of a second N_3^- to generate the dianion is endothermic in the gas phase so we do not give this energy.

The addition of CH_3CN to $MO_2(N_3)_2$ is an exothermic process for the isolated molecule (Figure 4). The CH_3CN group is in the equatorial plane for the pseudo-trigonal-bipyramidal structure with the N_3^- groups in the axial positions. The addition of the second CH_3CN goes into the same plane as the two M=O and the other CH_3CN with the two N_3^- groups perpendicular to the approximate plane. The binding energies for the addition of the first and second CH_3CN's are comparable at the MP2 level and are about 15 to 17 kcal mol^{-1}. Again, the W compound is slightly more Lewis acidic than the Mo compound. Axial addition of the first CH_3CN is 2.5 to 3.5 kcal mol^{-1} higher in energy than addition to the equatorial plane (Figure S1). The addition of the second CH_3CN giving a structure with one axial and one equatorial ligand is ca. 7 to 8 kcal mol^{-1} higher in energy and the addition with both CH_3CN axial is 18–19 kcal mol^{-1} higher in energy than when both are added to the equatorial position (Figure S1).

The observed and calculated vibrational data of the investigated molybdenum and tungsten dioxoazides are listed in the SI. The vibrational assignments are supported by the DFT calculations. The combined infrared and Raman spectra of $MoO_2(N_3)_2{\cdot}2\,CH_3CN$ are depicted in Figure S2. Bands due to the $\nu_{as}(N_3)$ vibration modes at about 2000–2150 cm^{-1} dominate the mid-infrared spectra of the metal dioxoazides. The bands of the $\nu_s(MO_2)$ and $\nu_{as}(MO_2)$ modes are observed in the ranges 900–960 cm^{-1} and 880–950 cm^{-1}, respectively, for the molybdenum compounds and 960–1000 cm^{-1} and 900–960 cm^{-1}, respectively, for the tungsten compounds. The Raman spectra of the investigated azides exhibit the strong bands of the $\nu_{as}(N_3)$ vibration modes in the region 2000–2150 cm^{-1} and the much weaker bands of the $\nu_s(N_3)$ modes at about 1200–1300 cm^{-1}, indicative for the presence of covalently bound azido groups. The bands due to the $M–N_{azide}$ stretching modes are observed at about 420–480 cm^{-1}. The presence of covalent azides was also confirmed with the help of ^{14}N NMR spectra. Solutions of all compounds exhibited resonances for N_α, N_β, and N_γ at about −260 ppm, −140 ppm, and −210 ppm, respectively, characteristic for covalent azido compounds.

The impact (IS) and friction sensitivities (FS) of the molybdenum(VI) and tungsten(VI) dioxoazides were determined using a BAM Fall Hammer and BAM Friction tester. The obtained sensitivity and stability data are summarized in Table S1 of the SI. The uncoordinated metal azides, $MoO_2(N_3)_2$ and $WO_2(N_3)_2$, as well as their acetonitrile adducts $MO_2(N_3)_2{\cdot}2\,CH_3CN$ are very sensitive to impact and friction ($IS \le 3$ J, $FS \le 20$ N) and have to be considered explosion hazards. Adduct formation with 2,2′-bipyridine or salt formation with PPh_4N_3 increases the stability of the metal dioxoazides enormously. Both 2,2′-bipyridine adducts, $(bipy)MoO_2(N_3)_2$ and $(bipy)WO_2(N_3)_2$ as well as $[PPh_4]_2[WO_2(N_3)_4]$ exhibit friction and impact sensitivities beyond the capabilities of our testers ($IS > 100$ J, $FS > 360$ N), whereas $[PPh_4]_2[MoO_2(N_3)_4]$ can still be considered insensitive with an IS of > 100 J and FS of 288 N. The thermal stabilities of most of the obtained azides were determined through differential thermal analysis (DTA) scans with heating rates of 5 °C min^{-1}. All studied metal dioxoazides showed smooth decompositions, and no explosions were observed upon heating at 5 °C min^{-1}. The solvent-free metal oxoazides, $MoO_2(N_3)_2$ and $WO_2(N_3)_2$, have decomposition onset temperatures of 145 °C and 155 °C, respectively. With onsets of 148 °C (Mo) and 150 °C (W), the acetonitrile adducts $MO_2(N_3)_2{\cdot}2\,CH_3CN$ decompose at almost identical temperatures as the solvent-free compounds. It is interesting to note that the DTA thermograms of both acetonitrile adducts show large, irreversible endotherms at about 100–110 °C, which presumably correspond to the loss of CH_3CN. The adduct formation with 2,2′-bipyridine raises the decomposition temperatures of the metal dioxodiazides to 160 °C ($(bipy)MoO_2(N_3)_2$) and 180 °C ($(bipy)WO_2(N_3)_2$). Not surprisingly, the salts $[PPh_4]_2[MoO_2(N_3)_4]$ and $[PPh_4]_2[WO_2(N_3)_4]$ show the highest thermal stabilities among the azido compounds of this study. Both salts melt about 15 °C before their decomposition temperatures of 200 °C (Mo) and 210 °C (W).

In conclusion, the first molybdenum(VI) and tungsten(VI) oxoazides have been prepared and characterized. $MoO_2(N_3)_2$ and $WO_2(N_3)_2$ have been obtained from the corresponding metal dioxodifluorides by their reactions with Me_3SiN_3. Whereas the fluoride–azide exchanges in acetonitrile solution resulted in the isolation of the solvated adducts $MO_2(N_3)_2{\cdot}2\,CH_3CN$, the solvent-free metal dioxodiazides were obtained when SO_2 was used as solvent. The reactions of $MO_2(N_3)_2$ with 2,2-bipyridine resulted in the formation of $(bipy)MoO_2(N_3)_2$ and $(bipy)WO_2(N_3)_2$, respectively. The hydrolysis of $(bipy)MoO_2(N_3)_2$ resulted in the formation and isolation of $[(bipy)MoO_2N_3]_2O$. The salts $[PPh_4]_2[MO_2(N_3)_4]$ (M = Mo, W) were obtained from the reactions of $MO_2(N_3)_2$ with two equivalents of PPh_4N_3. All molybdenum(VI) and tungsten(VI) dioxoazides were characterized by their vibrational spectra, impact, friction, and thermal sensitivity data, and, in the case of $(bipy)MoO_2(N_3)_2$, $(bipy)WO_2(N_3)_2$, $[PPh_4]_2[MoO_2(N_3)_4]$, $[PPh_4]_2[WO_2(N_3)_4]$, and $[(bipy)MoO_2N_3]_2O$ by their X-ray crystal structures.

Experimental Section

Caution! Polyazides are extremely shock-sensitive and can explode violently upon the slightest provocation. Because of the high energy content and the high detonation velocity of these azides, their explosions are particularly violent and can cause, even on a one mmol scale, significant damage. The use of appropriate safety precautions (safety shields, face shields, leather gloves, protective clothing, such as heavy leather welding suits and ear plugs) is mandatory. **Ignoring safety precautions can lead to serious injuries!**

Crystal structure determinations: The single-crystal X-ray diffraction data were collected on Bruker SMART or Bruker SMART APEX DUO diffractometers using Mo K_α radiation (graphite or TRIUMPH curved-crystal monochromator) from a fine-focus tube. Further crystallographic details can be obtained from the Cambridge Crystallographic Data Centre (CCDC, 12 Union Road, Cambridge CB21EZ, UK (Fax: (+44) 1223–336–033; e-mail: deposit@ccdc.cam.ac.uk) on quoting the deposition no. CCDC 1400348–1400352.

Computational Methods: The geometries were optimized at the density functional theory (DFT)[13] level with the LSDA (local spin density approximation) SVWN5[14] and hybrid B3LYP[15] exchange-correlation functionals with the DFT-optimized DZVP2 basis set[16] for H, C, N, and O atoms and the cc-pVDZ-PP[17] basis set for V using Gaussian 09 program system.[18] Vibrational frequencies were calculated to show that the structures were minima.

Keywords: crystal structures · molybdenum · oxoazides · polyazides · tungsten

How to cite: *Angew. Chem. Int. Ed.* **2015**, *54*, 9581–9585
Angew. Chem. **2015**, *127*, 9717–9721

[1] a) R. Haiges, R. J. Buszek, J. A. Boatz, K. O. Christe, *Angew. Chem. Int. Ed.* **2014**, *53*, 8200–8205; *Angew. Chem.* **2014**, *126*, 8339–8344, and references therein; b) W. P. Fehlhammer, W. Beck, *Z. Anorg. Allg. Chem.* **2013**, *639*, 1053–1082, and references therein; c) W. K. Seok, T. M. Klapötke, *Bull. Korean Chem. Soc.* **2010**, *31*, 781–788; d) T. M. Klapötke, *Chem. Ber. Recl.* **1997**, *130*, 443–451; e) I. C. Tornieporth-Oetting, T. M. Klapötke, *Angew. Chem. Int. Ed. Engl.* **1995**, *34*, 511–520; *Angew. Chem.* **1995**, *107*, 559–568; f) M.-J. Crawford, A. Ellern, R. Mayer, *Angew. Chem. Int. Ed.* **2005**, *44*, 7874–7878; *Angew. Chem.* **2005**, *117*, 8086–8090.

[2] a) R. Haiges, J. Boatz, A. Vij, V. Vij, M. Gerken, S. Schneider, T. Schroer, M. Yousufuddin, K. Christe, *Angew. Chem. Int. Ed.* **2004**, *43*, 6676–6680; *Angew. Chem.* **2004**, *116*, 6844–6848; b) R. Haiges, A. Vij, J. Boatz, S. Schneider, T. Schroer, M. Gerken, K. Christe, *Chem. Eur. J.* **2004**, *10*, 508–517.

[3] R. Haiges, P. Deokar, K. O. Christe, *Angew. Chem. Int. Ed.* **2014**, *53*, 5431–5434; *Angew. Chem.* **2014**, *126*, 5535–5538.

[4] R. Haiges, M. Vasiliu, D. A. Dixon, K. O. Christe, *Angew. Chem. Int. Ed.* **2015**, DOI: 10.1002/anie.201503985.

[5] R. Haiges, J. A. Boatz, R. Bau, S. Schneider, T. Schroer, M. Yousufuddin, K. O. Christe, *Angew. Chem. Int. Ed.* **2005**, *44*, 1860–1865.

[6] K. Dehnicke, J. Schmitte, D. Fenske, *Z. Naturforsch. B* **1980**, *35*, 1070–1074.

[7] R. Haiges, M. Rahm, K. O. Christe, *Inorg. Chem.* **2013**, *52*, 402–414.

[8] I. Sens, H. Stenger, U. Müller, K. Dehnicke, *Z. Anorg. Allg. Chem.* **1992**, *610*, 117–120.

[9] L. Arnaudet, R. Bougon, B. Ban, P. Charpin, J. Isabey, M. Lance, M. Nierlich, J. Vigner, *Can. J. Chem.* **1990**, *68*, 507–512.

[10] a) C. Møller, M. S. Plesset, *Phys. Rev.* **1934**, *46*, 0618–0622; b) J. A. Pople, J. S. Binkley, R. Seeger, *Int. J. Quantum Chem.* **1976**, 1–19.

[11] a) R. A. Kendall, T. H. Dunning, R. J. Harrison, *J. Chem. Phys.* **1992**, *96*, 6796–6806; b) K. A. Peterson, D. Figgen, M. Dolg, H. Stoll, *J. Chem. Phys.* **2007**, *126*, 124101; c) D. Figgen, K. A. Peterson, M. Dolg, H. Stoll, *J. Chem. Phys.* **2009**, *130*, 164108.

[12] S. G. Li, D. A. Dixon, *J. Phys. Chem. A* **2006**, *110*, 6231–6244.

[13] R. G. Parr, W. Yang, *Density-functional theory of atoms and molecules*, Oxford University Press, Clarendon Press, New York, Oxford, **1989**.

[14] a) J. C. Slater, *Quantum Theory of Molecules and Solids: The self-consistent field for molecules and solids*, McGraw-Hill, New York, **1963**; b) S. H. Vosko, L. Wilk, M. Nusair, *Can. J. Phys.* **1980**, *58*, 1200–1211.

[15] a) A. D. Becke, *J. Chem. Phys.* **1993**, *98*, 5648–5652; b) C. T. Lee, W. T. Yang, R. G. Parr, *Phys. Rev. B* **1988**, *37*, 785–789.

[16] N. Godbout, D. R. Salahub, J. Andzelm, E. Wimmer, *Can. J. Chem.* **1992**, *70*, 560–571.

[17] a) N. B. Balabanov, K. A. Peterson, *J. Chem. Phys.* **2005**, *123*, 084314; b) N. B. Balabanov, K. A. Peterson, *J. Chem. Phys.* **2006**, *125*, 074110.

[18] M. J. Frisch, G. W. Trucks, H. B. Schlegel, G. E. Scuseria, M. A. Robb, J. R. Cheeseman, G. Scalmani, V. Barone, B. Mennucci, G. A. Petersson, H. Nakatsuji, M. Caricato, X. Li, H. P. Hratchian, A. F. Izmaylov, J. Bloino, G. Zheng, J. L. Sonnenberg, M. Hada, M. Ehara, K. Toyota, R. Fukuda, J. Hasegawa, M. Ishida, T. Nakajima, Y. Honda, O. Kitao, H. Nakai, T. Vreven, J. A. Montgomery Jr., J. E. Peralta, F. Ogliaro, M. J. Bearpark, J. Heyd, E. N. Brothers, K. N. Kudin, V. N. Staroverov, R. Kobayashi, J. Normand, K. Raghavachari, A. P. Rendell, J. C. Burant, S. S. Iyengar, J. Tomasi, M. Cossi, N. Rega, N. J. Millam, M. Klene, J. E. Knox, J. B. Cross, V. Bakken, C. Adamo, J. Jaramillo, R. Gomperts, R. E. Stratmann, O. Yazyev, A. J. Austin, R. Cammi, C. Pomelli, J. W. Ochterski, R. L. Martin, K. Morokuma, V. G. Zakrzewski, G. A. Voth, P. Salvador, J. J. Dannenberg, S. Dapprich, A. D. Daniels, Ö. Farkas, J. B. Foresman, J. V. Ortiz, J. Cioslowski, D. J. Fox, Gaussian, Inc., Wallingford, CT, USA, 2009.

Received: May 22, 2015
Published online: July 14, 2015

